

# Numerical and experimental investigation of control performance of active mass damper system to high-rise building in use

S.J. Park and J. Lee

*R&D Technique Institute, Lotte Engineering and Construction Co. Ltd., Seoul 140-111, Korea*

H.J. Jung\* and D.D. Jang

*Department of Civil and Environmental Engineering, KAIST, Daejeon 305-701, Korea*

S.D. Kim

*Department of Civil, Environmental and Architectural Engineering, Korea Univ., Seoul 136-701, Korea*

*(Received October 16, 2008, Accepted April 10, 2009)*

**Abstract.** This paper numerically and experimentally investigates the control performance of the active mass damper (AMD) systems in a 26-story high-rise building in use. This is the first full-scale application of the AMD system for suppressing the wind-induced vibration of a building structure in Korea. In addition, the AMD system was installed on top of the building already in use, which may be the world's first implementation case. In order to simultaneously mitigate the transverse-torsional coupled vibration of the building, two AMD systems were applied. Moreover, the H-infinity control algorithm has been developed to utilize the maximum capacity of the AMD system. From the results of numerical simulation using the wind load obtained from the wind tunnel tests, it was found that the maximum acceleration responses of the building were reduced significantly. Moreover, the control performance of the installed AMD system was examined by carrying out the free and forced vibration tests. The acceleration responses on top of the building in the controlled case measured under strong wind loads were compared with those in the uncontrolled case numerically simulated by using the wind load deduced from the measured data and a structural model of the building. It is demonstrated that the AMD system shows good control performance in reducing the building accelerations.

**Keywords:** active mass damper; building in use; H-infinity control; wind-induced vibration mitigation.

---

## 1. Introduction

Recently, super high-rise buildings are competitively being constructed and planned over the world, especially in the regions of Middle East and East Asia (e.g., Buz Dubai in UAE and Taipei

---

\* Corresponding Author, E-mail: [hjung@kaist.ac.kr](mailto:hjung@kaist.ac.kr)

101 in Taiwan). A significant increase in the number of high-rise buildings leads the interest on structural control, because their dynamic characteristics such as inherent low damping ratios and low natural frequencies make high-rise buildings susceptible to strong winds. Although the strong winds do not affect the safety of building structures, they may cause undesirable vibration of buildings which makes the occupants discomfort. For these circumstances, the serviceability of the buildings has become an important part of building design.

In order to improve the serviceability of building structures, several measures have been developed so far. The traditional and simplest way is to increase the stiffness of the building so that its natural frequencies are shifted from the frequency range of wind excitation. However, it requires a large amount of materials and the cost problem may arise. Moreover, it cannot be a solution for buildings in use. An alternative way to solve the excessive vibration problem is to increase an effective damping ratio of the building by adding damping devices such as various configurations of steel dampers, visco-elastic dampers, viscous dampers, and mass control-type dampers of AMD (active mass damper), HMD (hybrid mass damper) and TMD (tuned mass damper). These damping devices can be categorized into two types depending on the requirement of the external power source such as passive control and active control. Passive-type devices have several advantages such as ease of maintenance, low price and guaranteed structural stability. However, those have also disadvantages of low performance, insufficient adaptability and so on. On the other hand, active-type devices, which are developed to overcome the disadvantages of passive-type dampers, have a high control efficiency, good adaptability and relative insensitivity to site conditions. Before 1980s, only a few active-type devices were adopted because there was doubt about control performance under severe disaster due to limitation of power source and undeveloped control algorithms, while many more passive-type devices were used (Kobori 1998, Sakamoto, *et al.* 1996). During the 1980s, active-type devices have been studied analytically and experimentally; and then, the active-type devices have become a main consideration for vibration control. In 1989, Kyobashi Seiwa building in Japan was equipped with AMD firstly in the world (Kobori, *et al.* 1991). Since then, more than 40 buildings have implemented active-type control systems (e.g., Datta 2003, Ikeda 2004). Although AMD is known that it is not good in event of extreme earthquakes, it has an excellent performance to events of strong winds or small to moderate earthquakes.

In July 2006, a discomfort during strong winds due to Typhoon Ewiniar was reported at the building which was completed in 2002. The building has five basement floors with SRC structural system and 26 floors with steel structure system, and which makes inherent low damping ratio. To figure out the reason of the occupants' discomfort, the preliminary field measurement was performed and additionally the wind tunnel test was carried out. From the results of tests, it was demonstrated that the accelerations of the building exceeded the acceleration criteria to ensure the serviceability (TE Solution 2007). The AMD system was selected to reduce the wind-induced vibration so that the serviceability of the building is assured. It is the first application of AMD for a residential building in Korea. Usually, the vibration control devices have been planned and implemented during construction stage. In this study, on the other hand, the AMD system was implemented to the building in use and this may be the first full-scale application of the AMD system to the building in use in the world. The two AMDs were implemented in June 2007 and the performance tests were also carried out.

This paper thoroughly investigates the control performance of the AMD system installed at the building in use by conducting a series of numerical simulations using the detailed structure model data and the estimated wind load as well as field tests such as free vibration tests and forced

vibration tests under typhoons. In numerical simulations, one of the robust control algorithms such as H-infinity control algorithm is used and occupants' comfort is examined according to AIJ (Architectural Institute of Japan) level. In the forced vibration tests under a typhoon, the controlled responses measured from accelerometers are compared with the uncontrolled responses calculated from numerical simulations using the estimated wind load and a structural model of the building.

## 2. Performance investigation of original building structure

### 2.1. Wind tunnel test

To determine the wind-induced accelerations of the original building structure, the high-frequency force balance test was performed with a scaled model using the boundary layer wind tunnel by TE Solution, Co., Ltd (TE Solution 2007). The wind tunnel is Eiffel-type and has a test section of 4.5 m (Width)  $\times$  2.5 m (Height)  $\times$  25 m (Length).

The building model and a proximity model of the surroundings for a radius of 300 m were made from balsa and rigid acrylic, respectively on a scale of 1:250. They are rotated to simulate the different wind directions at 10° intervals for the full 360° azimuth range. Fig. 1 shows the view of the scaled model under testing. The upstream terrain was modeled by roughness blocks to simulate the atmospheric wind corresponding to Category B in Korean Building Code (2005), which means urban and suburban areas, wooded areas, or other terrain with numerous closely spaced obstructions having the size of single-family dwellings or larger. Fig. 2 shows the vertical profiles of the mean wind speed and the longitudinal component of turbulence, measured just upstream of the proximity model. This figure indicates that the modeled wind represents well the expected full-scale wind at the actual site.

In the wind tunnel test, base shears, base moments and torsion were measured at 10° intervals for 36 wind directions. The spectra of the bending moments and torsion were calculated from the measured data. Estimates of the full scale responses for each wind direction, including the accelerations at the top occupied floor were calculated using random vibration theory by combining the measured wind loads on the scaled model, the spectra and dynamic properties of the building. The natural frequencies of the building were identified from preliminary field test (Daewoo Institute of Construction Technology 2006), and the diaphragm mass and mode shapes were provided by

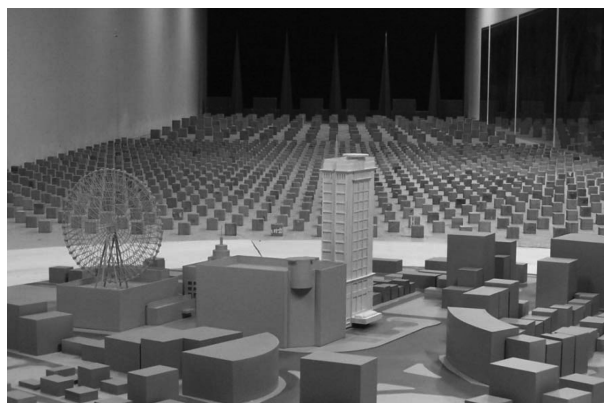


Fig. 1 Scaled model in boundary wind tunnel

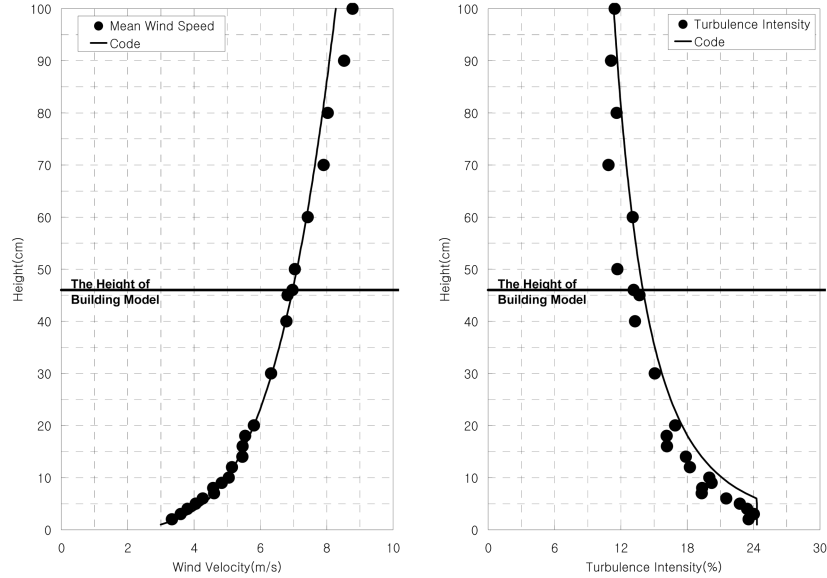


Fig. 2 Characteristics of the modeled wind

structural engineer. The generalized masses were calculated for the mode shapes with the mode value of the top occupied floor equal to unity. The structural damping values of 1% of critical were assumed for all three fundamental modes of vibration for the estimation of the accelerations.

## 2.2. Evaluation of habitability to building vibration

The habitability of the building was evaluated with the estimates of accelerations and Architectural Institute of Japan (AIJ) criteria. The accelerations were calculated at the top occupied floor which is 24th floor at a height of 96m above ground. AIJ criterion recommends that the maximum acceleration of a building should not exceed the value defined by Eq. (1) during the 10 consecutive minutes of a wind storm, for 1-year return period wind speed (AIJ 2004)

$$\alpha_{\max} = af^b \quad (1)$$

where  $f$  is the natural frequency of the structure,  $a$  and  $b$  are coefficients determined from Table 1.  $a$  and  $b$  are changed according to the natural frequency and habitability assessment level. The number in the habitability assessment level, the first column in Table 1, means the percentage of people who feel the vibration at each level.

Fig. 3 shows the peak acceleration at the top occupied floor. Torsional acceleration was expressed as linear acceleration at a distance 14.75 m, mass radius of gyration from the center of coordinates. For all direction, the acceleration along the X axis exceeds the criteria H-70, and for some directions, those along the Y and Z axes exceed the criteria H-50. The maximum accelerations of each direction, as shown in Fig. 4, indicate that the accelerations at the top occupied floor of the building may be higher than those of AIJ criterion. Therefore, a vibration reduction technique should be introduced to improve the habitability.

Table 1 Coefficients  $a$  and  $b$

Level	Natural Frequency	$0 \leq f \leq 1.5$		$1.5 \leq f \leq 2.5$	$2.5 \leq f \leq 10$	
		$a$	$b$	$a_{max}$	$a$	$b$
H-10		1.17		0.96	0.461	
H-30		1.67		1.37	0.658	
H-50		2.15	-0.5	1.76	0.846	0.8
H-50		2.76		2.26	1.806	
H-90		3.94		3.22	1.547	

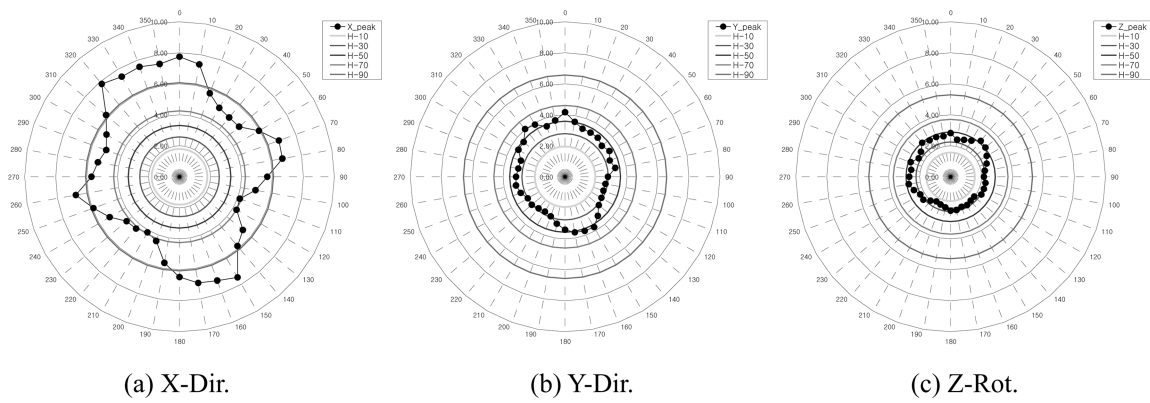


Fig. 3 Peak acceleration response (1-year return period)

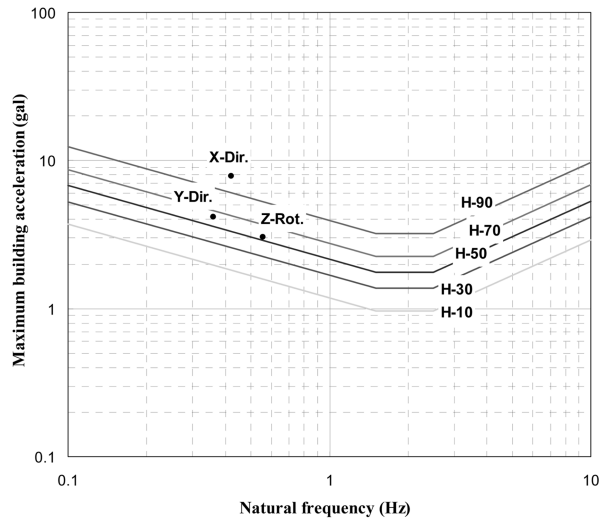


Fig. 4 Maximum accelerations with AIJ criterion

### 3. Composition and specification of AMD system

To suppress two translational and one rotational coupled vibrations of the building due to wind loads, two bi-directional AMD systems were implemented on the roof floor as shown in Fig. 5. The each AMD system is composed of two moving masses made of steel of 20 ton for X-direction and 10 ton for Y-direction, LM guides and blocks to guide the motion of masses, servo motors, control panels and two accelerometers for X- and Y-direction. Fig. 6 shows the detailed assembly drawing for the AMD system. As shown in the figure, the movements of masses are controlled by AC servo motors of two 45 kW for X-direction and one 22 kW for Y-direction. The stroke is limited to 60 cm on one side. A set of two accelerometers which are placed near each AMD measure the accelerometer of the building, and the AMD systems operate when the accelerometers of the building exceed the trigger level of 1.5 gal. The control panels provide the power of AC 380V and input signals to servo motors of AMD systems based on the designed control law and monitor the state of the AMD systems. The specifications of the AMD system are summarized in Table 2.

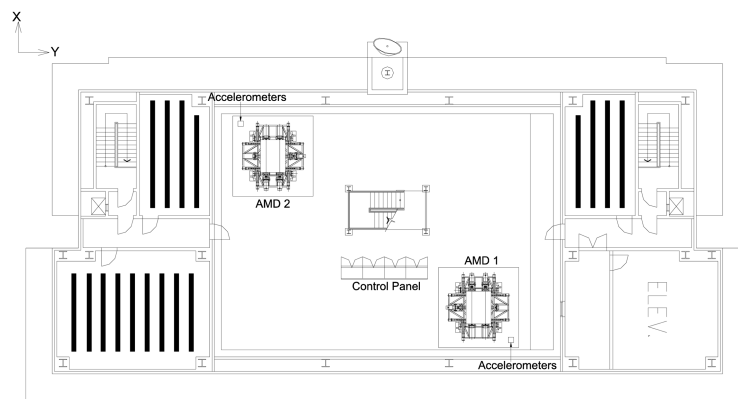


Fig. 5 Roof floor key-plan

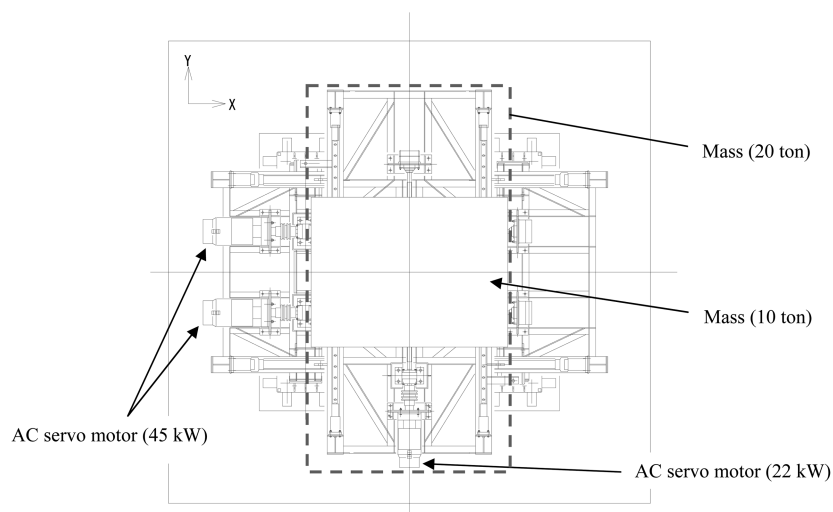


Fig. 6 Assembly drawing

Table 2 Specifications of AMD system

Item	Specification
Aspect	Bi-directional active mass type Total weight: 30 ton Size: 4.5 m(W) × 4.5 m(L) × 2.5 m(H)
Driving masses	Mass: 20 ton for X-direction 10 ton for Y-direction
Stroke	±60 cm
Driving type	AC servo motor: Two of 45 kW for X-direction One of 22 kW for Y-direction LM Guide: 2 guides per 1 LM rail
Power supply	AC380V 60Hz 3Φ4W 350kVA

### 4. Numerical verification

#### 4.1. Control system

In this study, the building is simplified as a single mass ( $m$ ) system with a spring element ( $k$ ) and a dashpot element ( $c$ ) shown in Fig. 7. First, only the control of the x-directional transverse-torsion coupled vibration is considered. The control of the y-directional transverse-torsion coupled vibration is exactly the same as the x-directional transverse-torsion case.

The equations of motion of the building with the AMD systems can be expressed as follows:

$$m \ddot{\eta}_x + c \dot{\eta}_x + k \eta_x = F_{wx} - F_{c1} - F_{c2} \tag{2}$$

$$m_\theta \ddot{\eta}_\theta + c_\theta \dot{\eta}_\theta + k_\theta \eta_\theta = F_{w\theta} - l_1 F_{c1} + l_2 F_{c2} \tag{3}$$

where  $m, c$  and  $k$  represent the modal mass, damping, stiffness, respectively.  $\eta$  is modal coordinate,  $F_w$  and  $F_c$  are external wind load and control force by AMD system and  $l$  is moment arm of AMD system from mass center of the building. Rewriting Eqs. (2) and (3) in state space expression, the following state equation is obtained

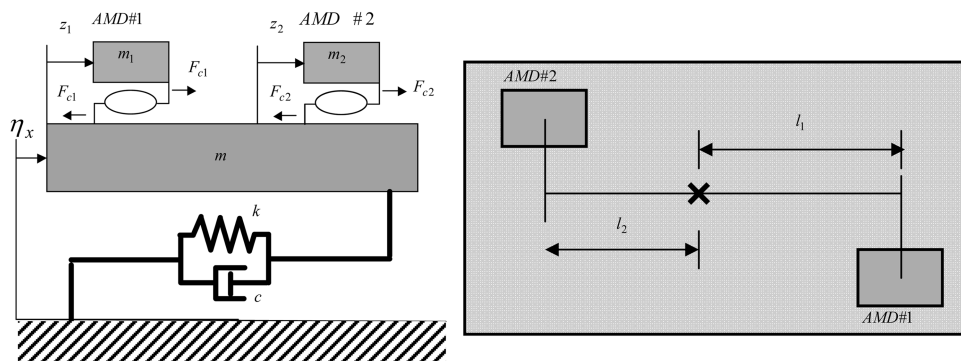


Fig. 7 Dynamic model of the building with AMD systems

$$\dot{X} = AX + Bu + Dw \quad (4)$$

$$y = [x_1 \ x_2 \ z_1 \ z_2]^T = CX + Ew \quad (5)$$

where  $w$  is the noise,  $x$  and  $z$  are the displacements of the building at roof floor and the AMD, respectively.

In this study, the H- $\infty$  controller is considered for the control algorithm of the AMD system. The controller is designed to control the first bending mode and the first torsion mode, and to stabilize the second mode or higher against each component of the bending and the torsion. The block diagram of the closed-loop system with a controller is shown in Fig. 8. A controller should be designed to satisfy the following inequality (Fujinami, *et al.* 2001):

$$\left\| \begin{array}{cc} W_1(s) & N(s) \\ W_2(s) & M(s) \end{array} \right\|_{\infty} < 1 \quad (6)$$

where  $N(s)$  and  $M(s)$  means the transfer function from external input to control input and from external force to output, respectively.

The weighting function for control input,  $W_u$ , has a high pass filter characteristic and is designed that has the highest gain around the second mode. The weighting function for building displacement at AMD,  $W_{zb}$ , is designed as a low pass filter that has the highest gain at the first mode and the weighting function for AMD displacement,  $W_{za}$ , is designed that has a high gain at low frequency level and a low gain at high frequency level considering the transfer function of AMD system. Fig. 9 shows gain plots of weighting functions.

#### 4.2. Numerical simulation results

To verify the effectiveness of the AMD system, a series of numerical simulations are performed. The external wind loads were calculated from the wind tunnel tests. Because the first mode is only considered, the wind load was generalized by the first mode for each direction. The 1-year return period wind load is considered and the wind directions are  $320^\circ$  and  $0^\circ$  for x- and y-direction,

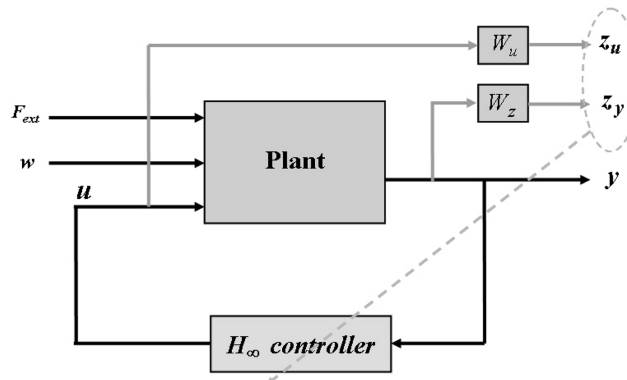


Fig. 8 Block diagram of closed-loop system

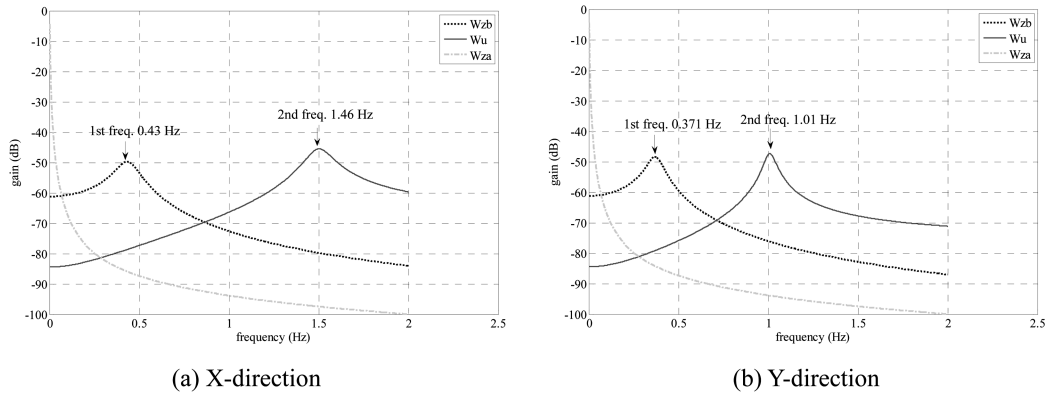


Fig. 9 Gain of weighting functions

respectively, where the building acceleration has the maximum value. The dynamic characteristics of the building, which were obtained from the detailed structural design model, are listed in Table 3 and the time histories of wind loads are shown in Fig. 10.

The results of numerical simulations are illustrated in Figs. 11 and 12. The graph in Fig. 11 shows the building accelerations of the uncontrolled and controlled cases. As shown in the figure, the maximum accelerations of the controlled case are reduced to 2.11 gal and 1.21 gal for x- and y-direction, respectively. Fig. 12 shows the maximum acceleration level comparisons with AIJ Standards. It is clearly demonstrated that the controlled case satisfies the criteria H-30 for x-direction and H-10 for y-direction, respectively.

Table 3 Dynamic characteristics of the building

Modal mass	X-translation: 4196 ton Y-translation: 4695 ton Torsion : 835710 ton-m
Natural frequency	X-translation: 0.421 Hz Y-translation: 0.360 Hz Torsion : 0.555 Hz

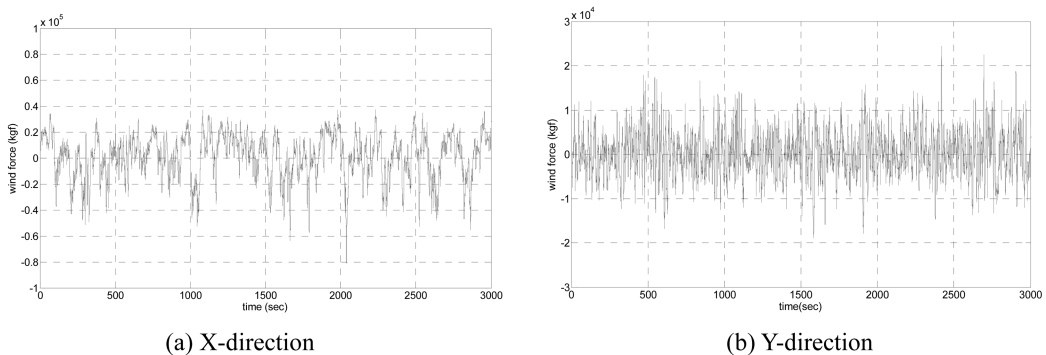


Fig. 10 Time history of wind load

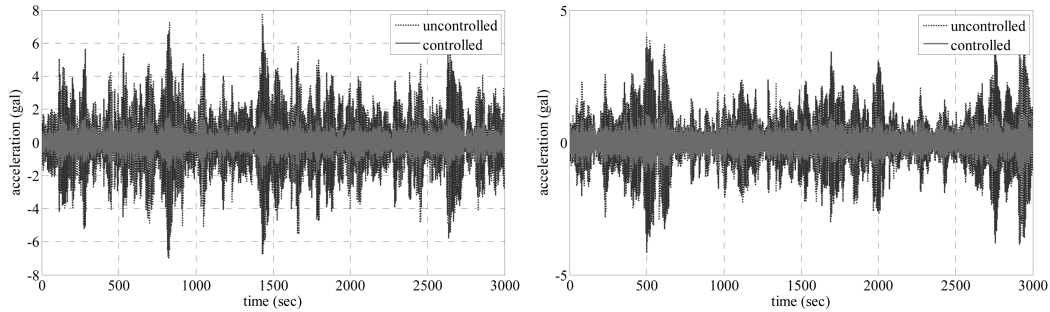


Fig. 11 Time history of building acceleration

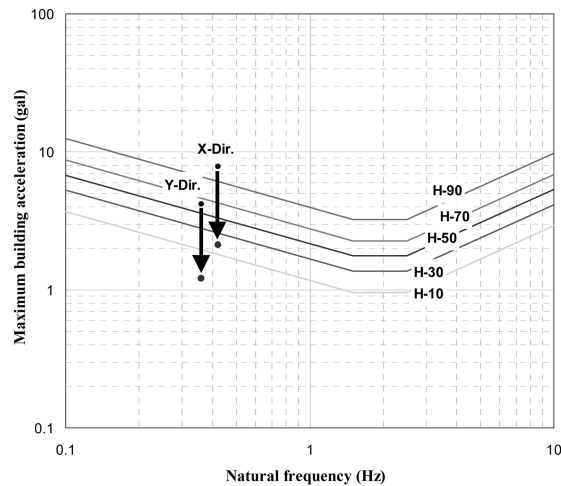


Fig. 12 Maximum acceleration level comparisons with AIJ criterion

## 5. Performance test results

To validate the effectiveness of the AMD system installed in the building, a series of the field tests of the AMD system such as the free vibration test and the forced vibration test under a typhoon are carried out.

### 5.1. Ambient vibration measurement

To investigate the natural frequencies of the building, the ambient vibration data was measured. Fig. 13 presents the time histories of the building responses and the FFT analysis result is shown in Fig. 14. From the ambient vibration measurement test, the first natural frequencies of the building are approximately 0.4375Hz for X-direction, 0.4Hz for Y-direction and 0.5875Hz for Z-rotational.

### 5.2. System Identification

To investigate the dynamic parameters of the building, the forced vibration tests were performed.

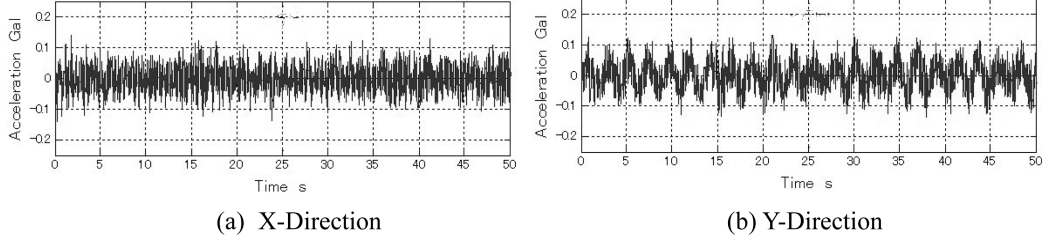


Fig. 13 Time history of the building response during the ambient vibration measurement

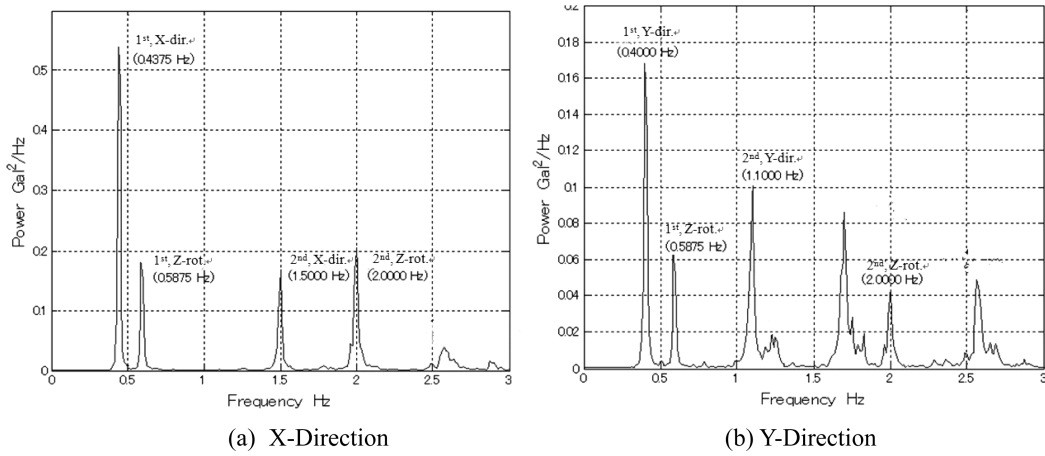


Fig. 14 Power spectral density of the building response during the ambient vibration measurement

The building was excited by the AMD.

Fig. 15 presents the dynamic model of the building which is considered as a 1 DOF model of only the first mode and AMD. The equation of motion can be written as follows:

$$\begin{aligned} m_1 \ddot{x}_1 + c_1 \dot{x}_1 + k_1 x_1 &= -f_c \\ m_2 (\ddot{x}_1 + \ddot{x}_2) &= f_c \end{aligned} \quad (7)$$

where,  $m_1$ ,  $c_1$ ,  $k_1$  and  $x_1$  are 1<sup>st</sup> modal mass, damping, stiffness and displacement of the building, respectively.  $f_c$  is the inertia force by the AMD. Eq. (7) can be rewritten as

$$(m_1 + m_2) \ddot{x}_1 + c_1 \dot{x}_1 + k_1 x_1 = -m_2 \ddot{z} \quad (8)$$

where,  $z$  is the AMD displacement.

The transfer function can be expressed by applying the Laplace transform to the Eq. (8).

$$\frac{X_1(s)}{m_2 s^2 Z(s)} = \frac{\ddot{X}_1(s)}{m_2 s^4 Z(s)} = \frac{1}{m_1 + m_2} \frac{1}{s^2 + 2\zeta_1 \omega_1 s + \omega_1^2} \quad (9)$$

where,  $s(=j\omega)$  is Laplace variable,  $\zeta_1$  and  $\omega_1$  are 1<sup>st</sup> modal damping and natural angular frequency, respectively.

From the forced vibration experiment using the AMD as an exciter, the measured transfer function

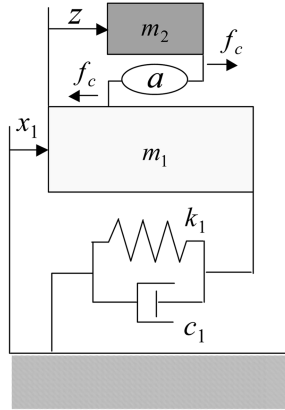


Fig. 15 Dynamic model of the building and AMD

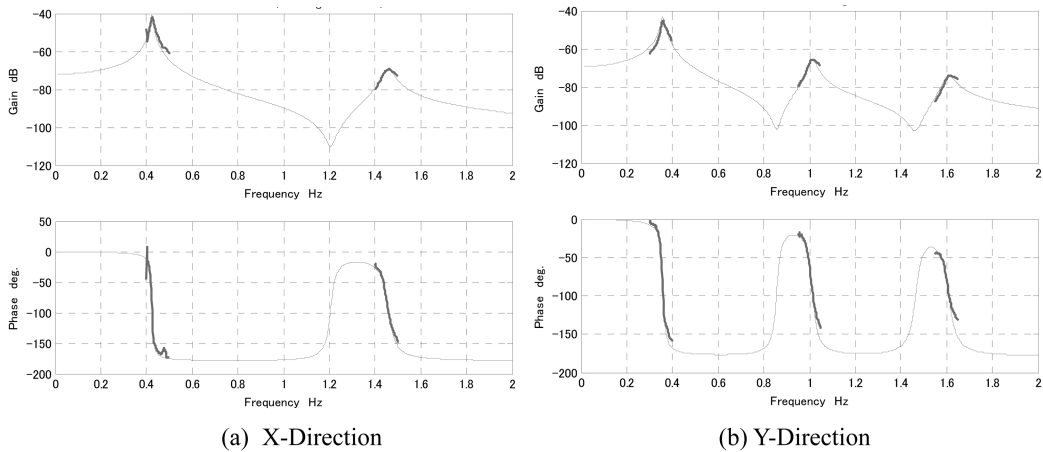


Fig. 16 Measured transfer function with simulated one

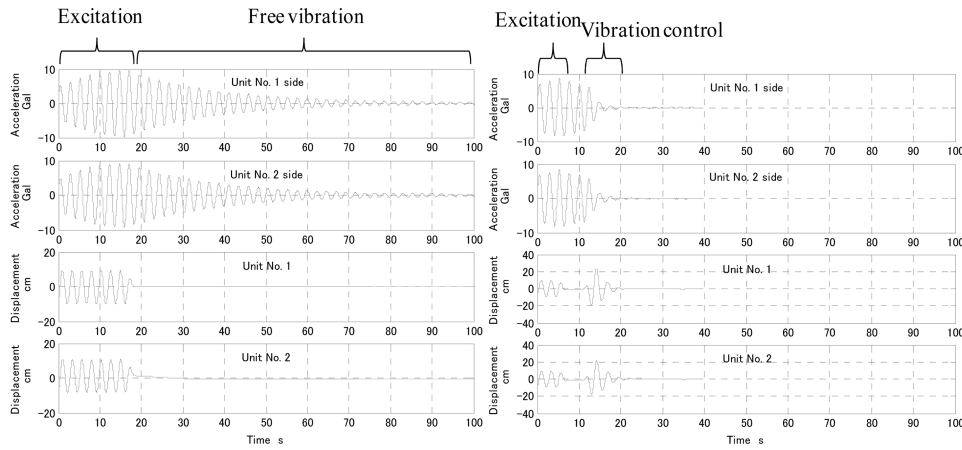
Table 4 Estimated dynamic parameters of the building

Mode	Natural frequency (Hz)	Damping ratio	Modal mass(ton)
X-dir. 1st	0.430	0.0136	$5.77 \times 10^3$
Y-dir. 1st	0.371	0.0234	$6.03 \times 10^3$

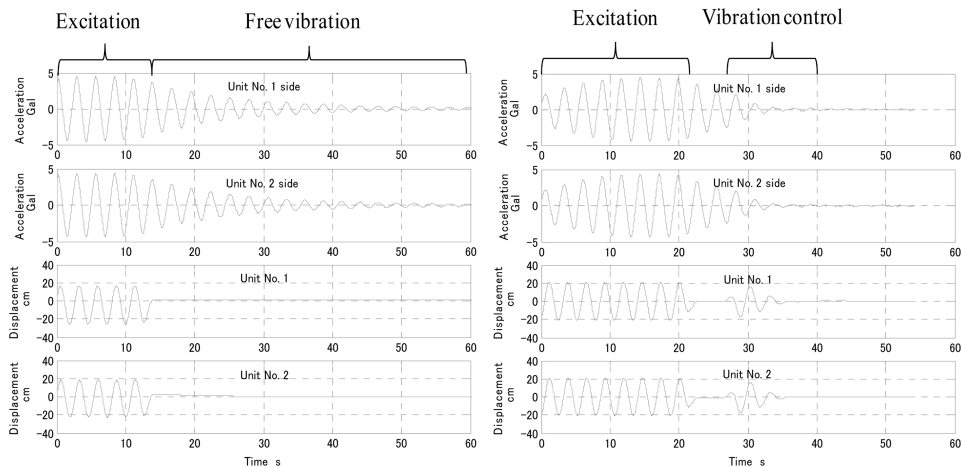
can be investigated. Then, the parameters of  $m_1$ ,  $\zeta_1$  and  $\omega_1$  can be estimated by curve fitting technique near the resonant frequency. Fig. 16 presents the transfer function of the building response with the simulated one. The estimated building parameters are shown in Table 4.

### 5.3. Free vibration test

To verify the control performance of the AMD, free vibration test was carried out in which the



(a) X-Direction



(b) Y-Direction

Fig. 17 Free vibration test

building was excited as a harmonic motion of the first mode by the AMD. Fig. 17 shows accelerations of the building and displacement of the AMDs for the case of excitation at the first natural frequency of each direction. From the test results, the performance of the AMD system could be confirmed by increases of equivalent damping ratios from 1.36% and 1.66% to 16.4% and 13.9% for X- and Y-dir., respectively.

#### 5.4. Forced vibration test with strong winds

In order to more clearly verify the effectiveness of the AMD system, its control performance under a typhoon should be investigated through comparing the building responses in the controlled case with those in the uncontrolled case. After the completion of the installation of AMD system, there was only one typhoon which affected the building so that the AMD system was operated to

reduce the vibration. Fig. 18 shows the measured acceleration responses at the roof floor during the Typhoon NARI on September 16, 2007. As shown in the figures, at least one of the acceleration responses in X-direction or Y-direction exceeded the threshold level (i.e., 0.2 gal or 0.02 m/sec<sup>2</sup>) two times (Case 1 and Case 2). Fig. 19 represents the corresponding AMD displacement. As seen from the figures, the AMD system was operated two times to mitigate the responses of the building.

As shown in the above figures, the AMD system was operated during a short time. Therefore, the direct approach which can evaluate the performance of AMD by turning on and off the AMD system cannot be applied. Instead, the indirect method which means the numerical simulation for the uncontrolled case was carried out. The wind loads acting on the building can be estimated by using the observed responses of the building and two AMD systems as well as the dynamic properties of the building (Nagashima, *et al.* 2001).

### 5.5. Estimation of wind loads

The dynamic equation of motion of the building in which the wind loads are acting on can be written as follows:

$$M\ddot{x} + C\dot{x} + Kx = EU + Dw \quad (10)$$

where  $M$ ,  $C$ ,  $K$  are mass, damping and stiffness matrix of the building, respectively;  $x = [x_1 \ x_2 \ \dots \ x_{26}]^T$

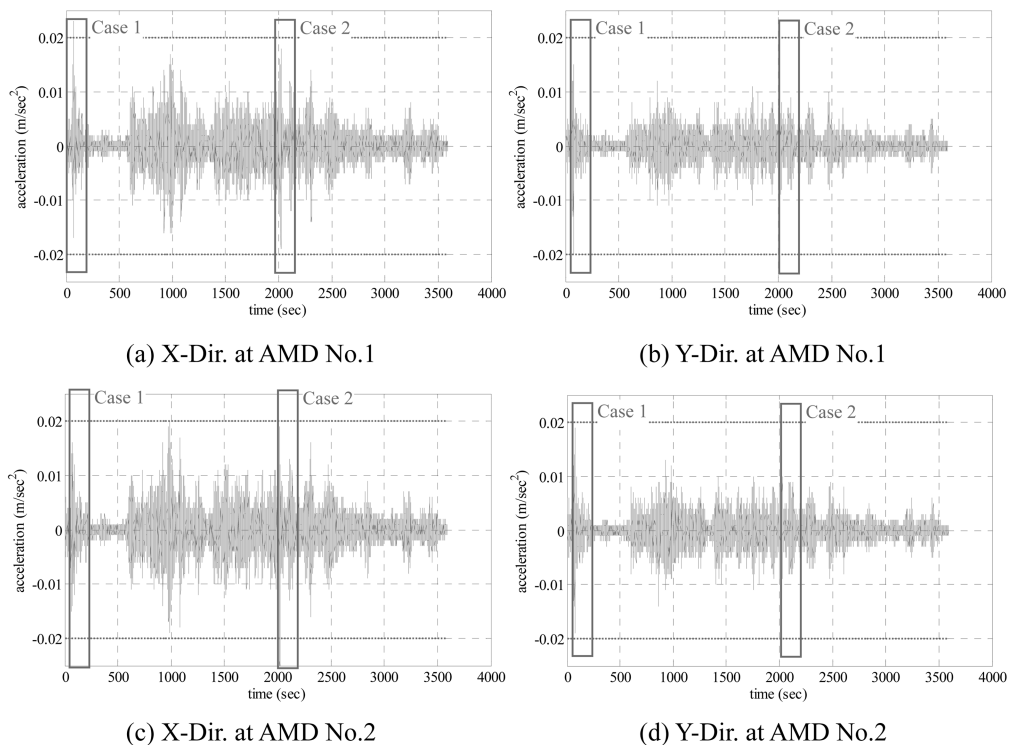


Fig. 18 Acceleration response at the roof floor during strong wind on Sep. 16, 2007

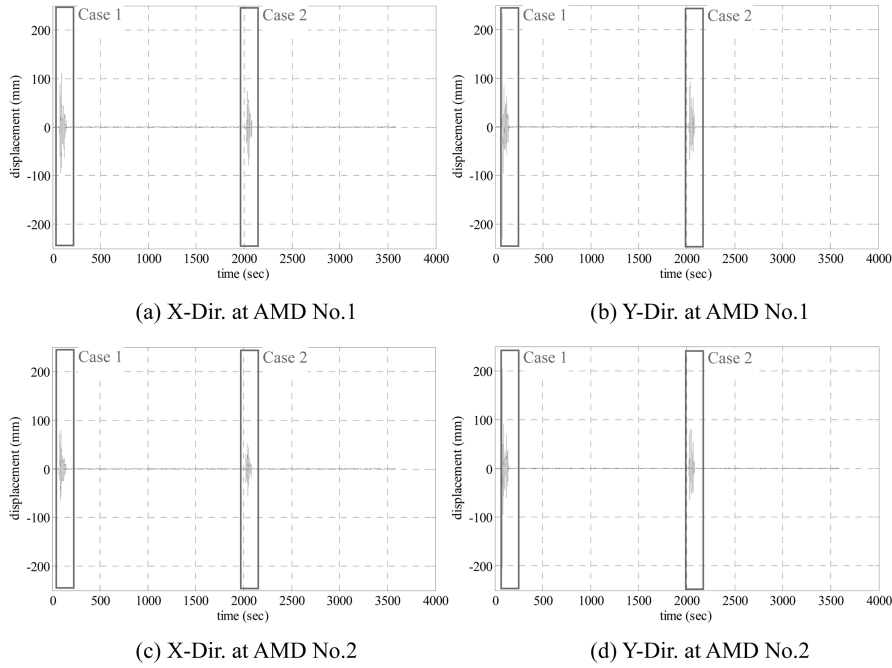


Fig. 19 Displacement response of AMD

is the displacement of the building;  $E = [0 \ 0 \ \dots \ 0 \ 1]^T$  is a constant matrix defining the location, 26<sup>th</sup> floor, of the control forces by the AMD system;  $U$  is the control forces by AMD which are calculated by multiplying the moving mass and accelerations of the AMDs;  $D = [d_1 \ d_2 \ \dots \ d_{26}]^T$  is a constant matrix defining the distribution of the wind loads;  $w$  is the assumed wind loads.

The  $i$ -th element of the distribution vector of the wind loads is obtained to be proportional to the surface area as follows:

$$d_i = z_i^{2\alpha} \times \Delta z_i \times \text{width}_i \quad (11)$$

where  $z_i$  and  $\Delta z_i \times \text{width}_i$  are the height at each floor and the surface area related to each floor, respectively. The power law exponent of wind speed,  $\alpha$ , is determined from the site roughness and the roughness of the actual site of the building is assumed as  $B$  (TE Solution 2007). According to the Standard Design Loads for Buildings of Korea (KBC 2005), the power law exponent of wind speed for the roughness  $B$  is 0.22.

To evaluate the control performance of the AMD system, the only 1<sup>st</sup> modes of each direction were used. The displacement of the building can be defined as the combination of normal mode and generalized coordinate as follows:

$$x_i = \varphi(i) \times q(t) \quad (12)$$

where  $\varphi$  is the normalized mode shape so that  $\varphi^T M \varphi = I$ , and  $q$  is the generalized coordinate. Substituting Eq. (12) into Eq. (10), the following dynamic equation of motion of modal coordinate can be obtained:

$$M\varphi\ddot{q} + C\varphi\dot{q} + K\varphi q = EU + Dw \quad (13)$$

By pre-multiplying  $\varphi^T$ , we have

$$\varphi^T M \varphi \ddot{q} + \varphi^T C \varphi \dot{q} + \varphi^T K \varphi q = \varphi^T E U + \varphi^T D w \quad (14)$$

$$\ddot{q} + 2\zeta\omega\dot{q} + \omega^2 q = E'U + D'w \quad (15)$$

in which  $\zeta$  and  $\omega$  are the damping ratio and the natural frequency of the building, respectively.

From Eq. (12), the modal responses of the building can be approximated from the responses at the 26<sup>th</sup> floor as follows:

$$\begin{aligned} q(t) &= \varphi^{-1}(26) \times x_{26} \\ x_{26} &= \varphi(26) \times q(t) \Rightarrow \dot{q}(t) = \varphi^{-1}(26) \times \dot{x}_{26} \\ \ddot{q}(t) &= \varphi^{-1}(26) \times \ddot{x}_{26} \end{aligned} \quad (16)$$

Substituting Eq. (16) into Eq. (15), the wind loads can be estimated as follows:

$$\varphi^{-1}(26)\ddot{x}_{26} + 2\zeta\omega\varphi^{-1}(26)\dot{x}_{26} + \omega^2\varphi^{-1}(26)x_{26} = E_e U + F_e w \quad (17)$$

By rearranging Eq. (17), the wind load is

$$w = D'^{-1}[\varphi^{-1}(26)\ddot{x}_{26} + 2\zeta\omega\varphi^{-1}(26)\dot{x}_{26} + \omega^2\varphi^{-1}(26)x_{26} - E'U] \quad (18)$$

In Eq. (18), the mode shapes of the building were provided by a structural engineer and the dynamic properties of the building were identified already.

The estimated wind loads for Cases 1 and 2 are shown in Fig. 20, which are derived from the acceleration at the roof floor of the building and the displacement of the AMD system. The static components were excluded by removing the averages.

### 5.6. Control performance of AMD

The accelerations of the building in the controlled case were back-calculated by substituting the estimated wind loads into the state-space equation of the building with the AMD system. Fig. 21 presents the simulated accelerations of the building compared with the measured responses, in which the simulated responses are match well with the measured responses. It can be seen that the identified building model is well-investigated.

The accelerations of the building in the uncontrolled cases were calculated by substituting the wind loads estimated as above and the AMD control forces of zero into Eq. (12). Fig. 22 shows the time histories and the power spectrums of the simulated accelerations of the building without control, as compared to the measured accelerations with control. As shown in the figures, the AMD system significantly reduces the maximum acceleration in all directions. Although the movement of the AMD system did not last for a long time and the accelerations of the building were small, it was demonstrated from the test that the AMD system performed well.

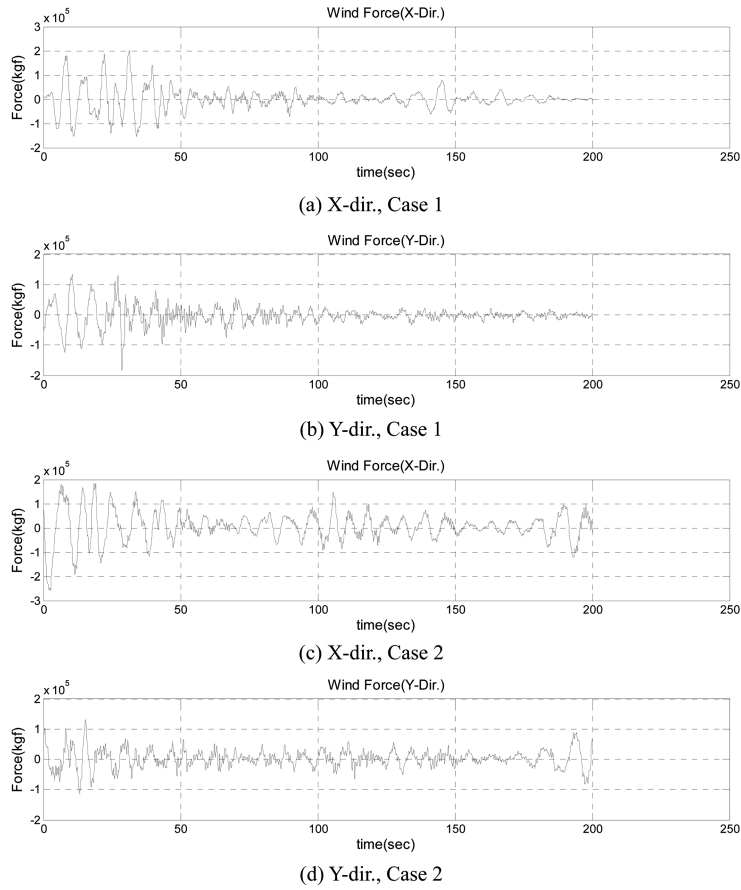


Fig. 20 Estimated wind loads

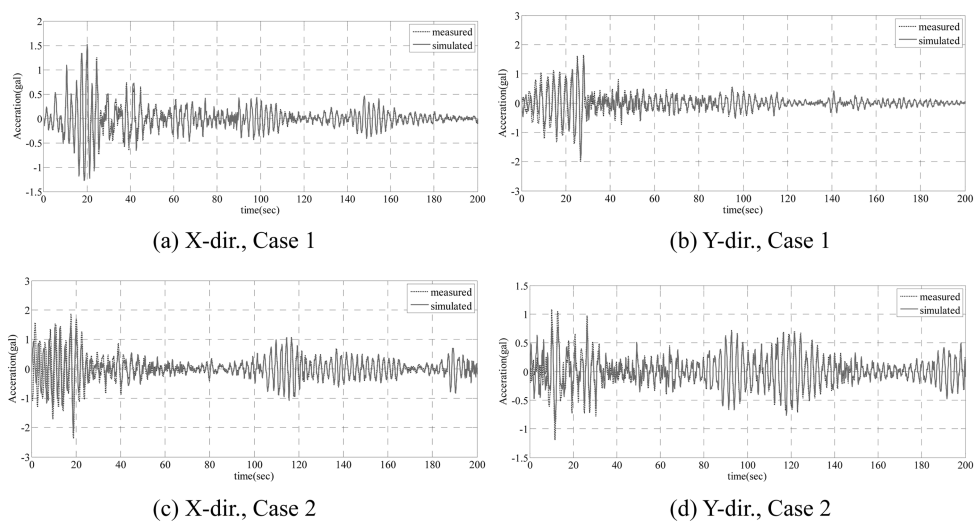
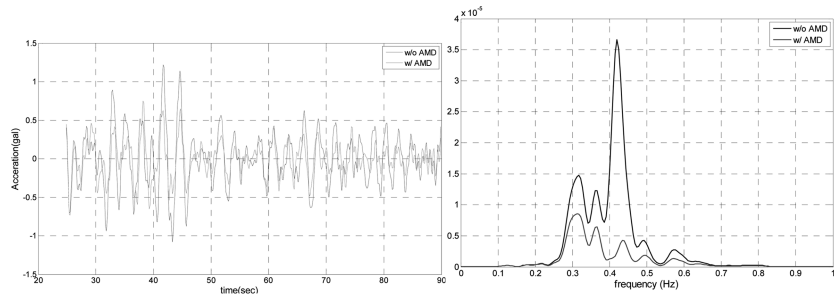
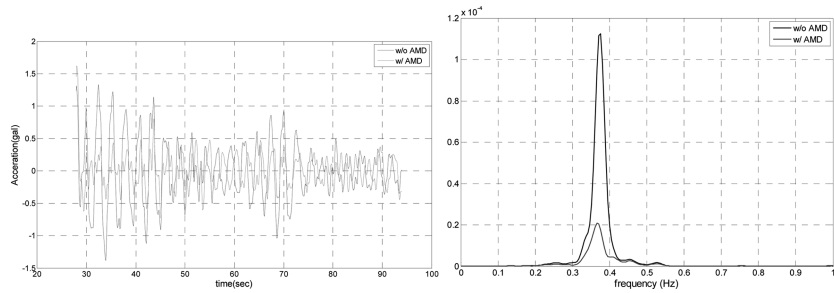


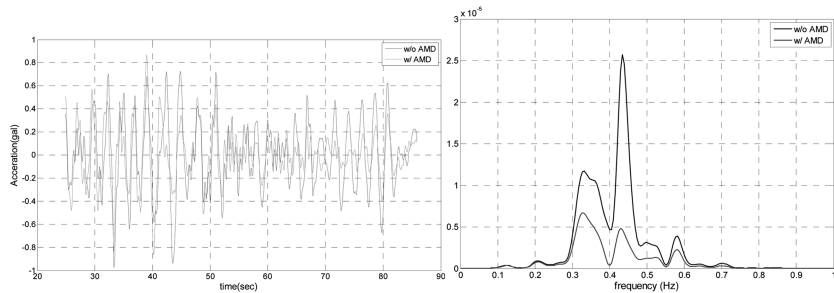
Fig. 21 Comparison of the simulated and measured responses of the building



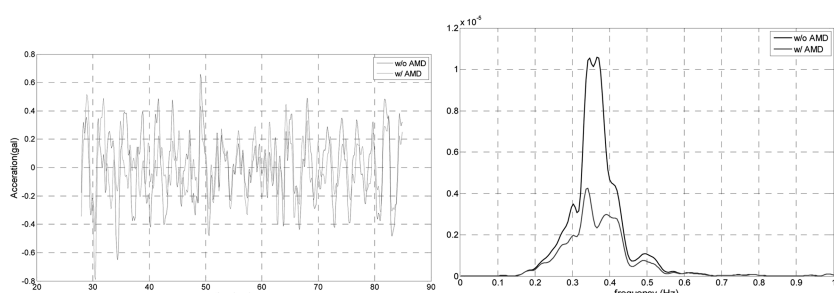
(a) X-dir., Case 1



(b) Y-Dir., Case 1



(c) X-dir., Case 2



(d) Y-dir., Case 2

Fig. 22 Time histories and spectrums of the building accelerations

## 6. Conclusions

In this study, the control performance of the AMD system which was recently applied to a 26-

story high-rise building in Korea has been thoroughly investigated. This is the first implementation of the AMD system for suppressing the wind-induced vibration of the residential building in Korea. Moreover, the application of AMD to the building in use may be the first case in the world. The AMD system employing H-infinity control algorithm shows the very good control performance in numerical simulations. Moreover, experimental tests such as the free and forced vibration analyses have been carried out. In the free vibration test, the damping ratio of the controlled case is much larger than that of the uncontrolled case. For the forced vibration test, the wind load was estimated from the measured responses of the building and the AMD system. It was used to calculate the accelerations of the building without control. Through a series of the performance tests, it was verified that the AMD system can mitigate the unacceptable vibrations significantly. To more clearly verify the effectiveness of the AMD system, however, additional tests should be carried out.

## Acknowledgements

The authors gratefully acknowledge the financial support of this research by Lotte Engineering and Construction, Co., Ltd. The performance tests of the AMD system was partially made in collaboration with IHI Corporation (Especially, Dr. Yuji Koike), who manufactured the AMDs described in this paper.

## References

- Architectural Institute of Japan (AIJ) (2004), *Guidelines for the Evaluation of Habitability to Building Vibration* (in Japanese).
- Daewoo Institute of Construction Technology (2006), "Measurement of Structural Responses of L Hotel under Wind Load", Technical report (in Korean).
- Datta, T.K. (2003), "A state-of-the-art review on active control of structures", *ISET Journal of Earthquake Technology*, **40**(1), 1-17.
- Fujinami, T., Saito, Y., Morishita, M., Koike, Y. and Tanida, K. (2001), "A hybrid mass damper system controlled by H-inf control theory for reducing bending-torsion vibration of an actual building", *Earthq. Eng. Struct. D.*, **30**(11), 1639-1653.
- Ikeda, Y. (2004), "Active and semi-active control of buildings in Japan", Special issue on "Some recent earthquake engineering research and practice in Japan", *Journal of the Japan Association for Earthquake Engineering*, **4**(3), 278-282 (CD-ROM).
- Kobori, T. (1998), "Mission and perspective towards future structural control research", *Proc. of the 2nd World Conf. on Structural Control*, 25-34.
- Kobori, T., Koshika, N., Yamada, K. and Ikeda, Y. (1991), "Seismic-response-controlled structure with active mass driver system. Part 1: Design", *Earthq. Eng. Struct. D.*, **20**(1), 133-149.
- Kobori, T., Koshika, N., Yamada, K. and Ikeda, Y. (1991), "Seismic-response-controlled structure with active mass driver system. Part 2: Verification", *Earthq. Eng. Struct. D.*, **20**(1), 151-166.
- Nagashima, I., Maseki, R., Asami, Y., Hirai, J. and Abiru, H. (2001), "Performance of hybrid mass damper system applied to a 36-storey high-rise building", *Earthq. Eng. Struct. D.*, **30**(11), 1615-1637.
- Nasu, T., Kobori, T., Takahashi, M., Niwa, N. and Ogasawara, K. (2001), "Active variable stiffness system with non-resonant control", *Earthq. Eng. Struct. D.*, **30**(11), 1597-1614.
- Nishitani, A. and Inoue, Y. (2001), "Overview of the application of active/semiactive control of building structures in Japan", *Earthq. Eng. Struct. D.*, **30**(11), 1565-1574.
- Sakamoto, M. and Kobori, T. (1996), "Applications of structural response control (reviews from the past and issues toward the future)", *Proc. of the 2nd Int. Workshop on Structural Control*, 470-481.
- Saito, T., Shiba, K. and Tamura, K. (2001), "Vibration control characteristics of a hybrid mass damper system

- installed in tall buildings”, *Earthq. Eng. Struct. D.*, **30**(11), 1677-1696.
- TE Solution (2007), “Wind tunnel test on L-building”, Technical report (in Korean).
- Watakabe, M., Tohdo, M., Chiba, O., Izumi, N., Ebisawa, H. and Fujita, T. (2001), “Response control performance of a hybrid mass damper applied to a tall building”, *Earthq. Eng. Struct. D.*, **30**(11), 1655-1676.

CC